Fast Multi-contrast MRI Reconstruction

Junzhou Huang[1], Chen Chen[1], and Leon Axel[2]

[1] Department of Computer Science and Engineering, University of Texas at Arlington, TX, USA 76019
[2] Department of Radiology, New York University, New York, NY 10016

Abstract. This paper proposes an efficient algorithm to simultaneously reconstruct multiple T1/T2-weighted images of the same anatomical cross section from partially sampled k-space data. The simultaneous reconstruction problem is formulated as minimizing a linear combination of three terms corresponding to a least square data fitting, joint total-variation (TV) and group wavelet-sparsity regularization. It is rooted in two observations: 1) the variance of image gradients should be similar for the same spatial position across multiple contrasts; 2) the wavelet coefficients of all images from the same anatomical cross section should have similar sparse modes. To efficiently solve this formulation, we decompose it into group sparsity and joint TV regularization subproblems, respectively. Finally, the reconstructed image is obtained from the weighted average of solutions from two subproblems in an iterative framework. We compare the proposed algorithm with previous methods on SRT24 multi-channel Brain Atlas Data. Experiments demonstrate its superior performance for multi-contrast MR image reconstruction.

1 Introduction

Magnetic Resonance Imaging (MRI) has been widely used to image the same anatomical cross section under multiple contrast settings, since the multi-contrast MRI can achieve superior power for clinical diagnosis over individual T1, T2 or proton-density weighted images.

Recent developments in compressive sensing (CS) theory [1] show that accurate MRI reconstruction can be achieved from highly undersampled k-space data. Motivated by the CS theory, Lustig et al. [2] proposed their pioneering work SparseMRI for CS-MRI. They showed that the combination of gradient and wavelet sparsity is far better than each of them separately in CS-MRI. However, their method based on conjugate gradient (CG) is not fast enough for practical MR images. Operator-splitting (TVCMRI [3]) and variable splitting (RecPF [4]) techniques were proposed then to accelerate this problem. Both of them gain time savings over the SparseMRI [2]. Recently, a composite splitting algorithm (FCSA [5] [6]) further accelerated this problem with convergence guarantee $\mathcal{O}(1/\sqrt{\varepsilon}))$, where ε is the accuracy. It was the best algorithm among ones that were tested.

All above introduced methods are designed for individual MR image reconstruction. When they are directly applied to each of multi-contrast MR

images, the CS theory guides us that the necessary measurement number is $\mathcal{O}(TK + TKlog(n/K))$ [1], where T is the contrast number, K is the sparsity number and n is the pixel number. However, the multi-contrast MR images are not independent but highly correlated. If one of them has smaller values in wavelet or gradient domain in a spatial position, all of them should likely have smaller values in wavelet or gradient domain for the same position. So, they should be group sparse on wavelet or gradient domain, not only standard sparse. According to the group sparsity theory for CS [7], the necessary measurement number can be reduced to $\mathcal{O}(TK + Klog(n/K))$ instead of $\mathcal{O}(TK + TKlog(n/K))$.

Unfortunately, no work has fully utilized these benefits so far. In [8], group sparsity is exploited on wavelet coefficients of multi-contrast MR images to achieve better results than standard sparsity. However, they did not consider the group sparsity on gradients. In [9], group sparsity on gradients of multi-contrast MRI is exploited under a multi-task Bayesian framework [10]. However, it is unknown how to couple group wavelet-sparsity into their method. Intuitively, better performance can be achieved by fully exploiting group sparsity on both wavelet and gradient domains for multi-contrast MRI.

This paper proposes an efficient algorithm to further accelerate multi-contrast MRI by fully exploiting the group sparsity on both wavelet and gradient domain over multi-contrast. The reconstruction problem is formulated as minimizing a linear combination of three terms corresponding to a least square data fitting, joint total-variation (TV) and group wavelet-sparsity regularization. A novel algorithm FCSA-MT is developed to efficiently solve this problem. It can obtain an ϵ-optimal solution in $\mathcal{O}(1/\sqrt{\epsilon})$ iterations. Extensive experiments on Multi-contrast Brain MRI data demonstrate its superior performance over all previous methods in term of the reconstruction accuracy and computational complexity.

2 Related Work

2.1 Compressed Sensing MRI

The CS MRI [2][3][4][5] can be formulated as follows:

$$\hat{x} = \arg\min_x \{\frac{1}{2}\|Rx - b\|^2 + \alpha\|x\|_{TV} + \beta\|\Phi x\|_1\} \quad (1)$$

where α and β are two positive parameters, b is the undersampled measurements of k-space data, R is a partial Fourier transform, Φ is a wavelet transform and x denotes the MR image. The TV was defined discretely as $\|x\|_{TV} = \sum_{i=1}^{n} \sqrt{((\nabla_1 x_i)^2 + (\nabla_2 x_i)^2)}$ where ∇_1 and ∇_2 denote the forward finite difference operators on the first and second coordinates, respectively. Several classic methods have been proposed to attack this problem, including CG [2], TVCMRI [3], RecPF [4] and FCSA [5]. As far as we know, the FCSA is the best in terms of both reconstruction accuracy and computational complexity.

The FCSA [5] solves the problem :$\min_x\{F(x) \equiv f(x)+g_1(x)+g_2(x), x \in \mathbf{R^n}\}$, where f is a smooth convex function with Lipschitz constant L_f, and $g_{i=1,2}$ are

Algorithm 1 FCSA [5]

Input: $\rho = \frac{1}{L_f}$, α, β, $t^1 = 1$ $z = x^0$
for $k = 1$ **to** N **do**
$y = z - \rho \nabla f(z)$
$x_1 = \arg\min_x \{\frac{1}{4\rho}\|x-y\|^2 + \alpha\|x\|_{TV}\}$
$x_2 = \arg\min_x \{\frac{1}{4\rho}\|x-y\|^2 + \beta\|\Phi x\|_1\}$
$x^k = \frac{x_1+x_2}{2}$; $t^{k+1} = \frac{1+\sqrt{1+4(t^k)^2}}{2}$
$z = x^k + \frac{t^k-1}{t^{k+1}}[x^k - x^{k-1}]$
end for

Algorithm 2 Proposed FCSA-MT

Input: $\rho = \frac{1}{L_f}$, α, β, $t^1 = 1$ $z_s = x^0$
for $k = 1$ **to** N **do**
$Y(:,s) = z_s - \rho \nabla f_s(z_s)$, $s = 1, \ldots, T$
$X_1 = \arg\min_X \{\frac{1}{4\rho}\|X - Y\|^2 + \alpha\|X\|_{JTV}\}$
$X_2 = \arg\min_X \{\frac{1}{4\rho}\|X - Y\|^2 + \beta\|\Phi X\|_{2,1}\}$
$X^k = \frac{X_1+X_2}{2}$; $t^{k+1} = \frac{1+\sqrt{1+4(t^k)^2}}{2}$
$z_s = X^k(:,s) + \frac{t^k-1}{t^{k+1}}[X^k(:,s) - X^{k-1}(:,s)]$
end for

convex functions. $\nabla f(x)$ denotes the gradient of the function f at the point x. $x \in \mathbf{R}^n$ is called an ϵ-optimal solution to the problem if $F(x) - F(x^*) \leq \epsilon$ holds.

In the problem of CS-MRI, $f(x) = \frac{1}{2}\|Rx - b\|^2$, $g_1(x) = \alpha\|x\|_{TV}$ and $g_2(x) = \beta\|\Phi x\|_1$. Algorithm 1 outlines the FCSA. It can obtain an ϵ-optimal solution in $\mathcal{O}(1/\sqrt{\epsilon})$ iterations. Moreover, the cost of each iteration is $\mathcal{O}(n \log(n))$ in FCSA for problem (1).

2.2 Multi-contrast Reconstruction

Multi-contrast MRI reconstruction means the simultaneous reconstruction of multiple T1/T2-weighted MR images $\{x_s\}_{s=1}^T \in \mathbf{R}^n$ for the same anatomical cross section from partially sampled k-space data $\{b_s\}_{s=1}^T$. In [8], group sparsity is exploited on wavelet coefficients of multi-contrast MR images instead of standard sparsity. Its formulation is as follows:

$$\hat{X} = \arg\min_X \|\Phi X\|_{2,1}; \sum_{s=1}^{T} \|R_s X(:,s) - b_s\|^2 \leq \sigma^2 \tag{2}$$

where $X = [x_1, ..., x_T] \in \mathbf{R^{n \times T}}$ are multi-contrast images, and R_s is the measurement matrix of $m_s \times n$ for x_s. The L21 norm term was defined as $\|\Phi X\|_{2,1} = \sum_{i=1}^n (\sqrt{\sum_{s=1}^T (\Phi X_{is})^2})$. Then, the SPGL1 [11] is directly used to solve it. However, they did not consider the group sparsity on gradients (unknown how to add it into their framework).

In [9], group sparsity on gradients of multi-contrast MRI is exploited under a multi-task Bayesian framework [10]. In their work, the gradients of images are reconstructed from their measurements in k-space under a Bayesian framework. Their experiments show the advantage of group sparsity on gradients over conventional sparsity. However, due to the inherent shortcoming of Bayesian frameworks, their method is very slow. It is also unknown how to couple group wavelet-sparsity into their method.

Algorithm 3 Proposed FJGP for Joint Total Variation

Input: ρ,α, Y, $(R_s, S_s) = (P_s, Q_s) = (\mathbf{0}_{(n_1-1)\times n_2}, \mathbf{0}_{n_1\times(n_2-1)})$
for $k = 1$ **to** N **do**
  $t^{k+1} = \frac{1+\sqrt{1+4(t^k)^2}}{2}$
  for $s = 1$ **to** T **do**
    $(P_s^k, Q_s^k) = \mathbb{P}_p[(R_s, S_s) + \frac{1}{16\rho\alpha}\mathcal{L}^T\mathbb{P}_C[Y(:,s) - 2\rho\alpha\mathcal{L}(R_s, S_s)]]$
    $(R_s, S_s) = (P_s^k, Q_s^k) + \frac{t^k-1}{t^{k+1}}(P_s^k - P_s^{k-1}, Q_s^k - Q_s^{k-1})$
  end for
end for
$X(:,s) = \mathbb{P}_C[Y(:,s) - 2\rho\alpha\mathcal{L}(P_s^K, Q_s^K)]$ for $i = 1, ..., T$

3 Fast Multi-contrast Reconstruction

3.1 Formulation and Algorithm

In the multi-contrast setting, the MR images denote MRI scans with different image weights.We have two observations about them: 1) the variance of image gradients should be similar for the same spatial position across multiple contrasts; 2) the wavelet coefficients of all MR images from the same spatial positions have similar sparse modes. Intuitively, better performance can be achieved by fully exploiting group sparsity on both wavelet and gradient domains for multi-contrast MRI. Motivated by these, the simultaneous reconstruction problem can be formulated as follows:

$$\hat{X} = \arg\min_X \{\frac{1}{2}\sum_{s=1}^{T}\|R_sX(:,s) - b_s\|^2 + \alpha\|X\|_{JTV} + \beta\|\Phi X\|_{2,1}\} \tag{3}$$

where α and β are two positive parameters, b_s is the undersampled measurements of k-space data for the s-th MR image $x_s = X(:,s)$, R_s is a partial Fourier transform for x_s and Φ is a wavelet transform. The JTV was defined discretely as $\|X\|_{JTV} = \sum_{i=1}^{n}\sqrt{\sum_{s=1}^{T}((\nabla_1 X_{is})^2 + (\nabla_2 X_{is})^2)}$. Algorithm 2 outlines the proposed algorithm for the multi-contrast reconstruction. Its efficiency is highly dependent on how quickly we can solve the second step and third step in each iteration. They correspond to two subproblems: JTV and group wavelet sparsity problem.

3.2 Group Wavelet Sparsity

The step 3 in Algorithm 2 is to solve the group wavelet sparsity problem:

$$\hat{X} = \arg\min_X \{\frac{1}{4\rho}\|X - Y\|^2 + \beta\|\Phi X\|_{2,1}\} \tag{4}$$

It has a closed form solution by the soft thresholding:

$$(\Phi\hat{X})_i = max(1 - \frac{2\rho\beta}{\|(\Phi Y)_i\|_2}, 0)(\Phi Y)_i \tag{5}$$

where $(\cdot)_i$ denotes the i-th row of the matrix for $i = 1, ..., n$.

3.3 Joint Total Variation

The step 2 in Algorithm 2 is to solve the JTV denoising problem:

$$X_1 = \arg\min_X \{\frac{1}{4\rho}\|X - Y\|^2 + \alpha\|X\|_{JTV}\} \tag{6}$$

As far as we know, there is no closed form solution for it. The Fast Gradient Projection (FGP) algorithm for TV [12] can not directly solve it, due to the different formulation. Fortunately, we can develop a new method, called Fast Joint-Gradient Projection (FJGP) algorithm, for this JTV problem by modifying the FGP algorithm in [12].

Algorithm 3 outlines the proposed FJGP. Due to page limitation, we follow the notations in FGP [12]. Please refer FGP [12] for more details. n_1 and n_2 denote the width and height of an image with $n_1 * n_2 = n$, $\mathcal{L}(P, Q)_{i,j,s} = P_{i,j,s} - P_{i-1,j,s} + Q_{i,j,s} - Q_{i,j-1,s}$ for $i \in [1, n_1]$, $j \in [1, n_2]$, $s \in [1, T]$. The $\mathcal{L}^T$ is defined as $\mathcal{L}^T(X) = (P, Q)$, where $P \in \mathbf{R}^{(n_1-1)\times n_2\times T}$ and $Q \in \mathbf{R}^{n_1\times(n_2-1)\times T}$. The $\mathbb{P}_p$ is a projection operator used to ensure that $\sum_{s=1}^{T}(P_{i,j,s}^2 + Q_{i,j,s}^2) \leq 1$, $|P_{i,n_2,s}| \leq 1$ and $|Q_{n_1,j,s}| \leq 1$. The $\mathbb{P}_C$ is a projection operator to ensure the reconstructed X stay in the constrained set C. The proposed FJGP algorithm has fast convergence performance, borrowed from the FGP [12]. It converges in $\mathcal{O}(1/\sqrt{\epsilon})$ iterations. The computation cost is $\mathcal{O}(Tn)$ in each iteration.

3.4 Convergence and Complexity

The proposed FCSA-MT algorithm has fast convergence performance, borrowed from the FCSA [5]. It can obtain an ϵ-optimal solution in $\mathcal{O}(1/\sqrt{\epsilon})$ iterations. The cost of each iteration in the proposed algorithm is $\mathcal{O}(Tn\log(n))$, as confirmed by the following observations. The steps 4 and 5 only involve adding vectors or scalars, and thus cost only $\mathcal{O}(Tn)$ or $\mathcal{O}(1)$. In step 1, $\nabla f_s(z_s) = R_s^T(R_s z_s - b_s)$, since $f_s(z_s) = \frac{1}{2}\|R_s z_s - b_s\|^2$ in this case. Thus, this step only costs $\mathcal{O}(Tn\log(n))$.The second step (JTV) can be quickly solved by the proposed FJGP with cost $\mathcal{O}(Tn)$; the third step (group wavelet sparsity) has a closed form solution and can be computed with cost $\mathcal{O}(Tn\log(n))$.

4 Experiments

4.1 Experiment Setup

Our experiments were conducted on the multi-contrast data extracted from the SRI24 Multi-Channel Brain Atlas Data [13]. The MR images were acquired

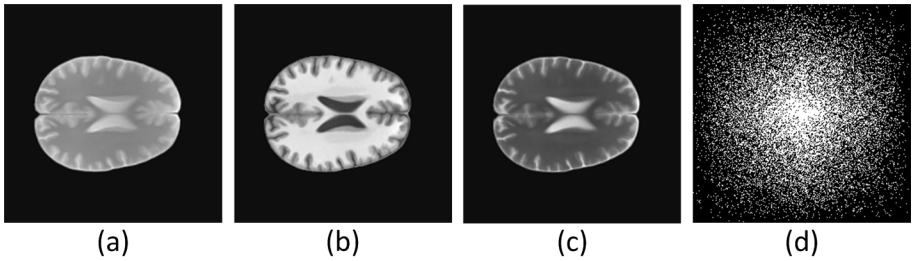

Fig. 1: SRI24 Multi-Channel Brain Atlas Data [13]: a) Proton density-weighted image; (b) T1-weighted image; (c) T2-weighted image and (d) Sampling mask.

with three different contrast settings at 3T: 1) Proton density-weighted images: they were acquired with a 2D axial dual-echo fast spin echo (FSE) sequence (TR=10,000 ms, TE=14 ms); 2) T1-weighted images: they were acquired with a 3D axial IR-prep Spoiled Gradient Recalled (SPGR) sequence, where TR=6.5 ms and TE=1.54 ms; and 3) T2-weighted images: they were acquired with the same sequence as the proton density-weighted scan. However, TE equals 98 ms in this case. The data includes 620 MR images with size 256×256 covering a 24-cm field-of-view.

The partial Fourier transform R_s in problem (3) consists of m_s rows of a $n \times n$ matrix corresponding to the full 2D discrete Fourier transform. The m_s selected rows correspond to the acquired b_s. The sampling ratio is defined as m_s/n. To randomly select rows in k-space, we randomly obtained more samples at low frequencies and less samples at higher frequencies. This sampling scheme is the same as those in [2][3][4][5] and has been widely used in CS-MRI. Figure 1 shows example images and the sampling mask.

All experiments were conducted on a 2.2GHz PC in Matlab environment. We compared the proposed FCSA-MT [3] with conventional CS-MRI methods (CG [2], TVCMRI [3], RecPF [4] and FCSA[5]) and two recent multi-contrast reconstruction methods (SPGL1 [8] and Bayesian [9]). For fair comparisons, the codes were obtained by downloading them from their websites or asking for them from the authors. We carefully followed their experiment setup. The regularization parameters α and β were set as 0.001 and 0.035.

4.2 Numerical Results

We first compared the proposed method with conventional CS-MRI methods on all images. The sample ratio was set to be approximately 25%. To perform fair comparisons, all methods ran 50 iterations, except that the CG ran only 8 iterations due to its higher complexity. To reduce the randomness, each experiment ran 100 times. Figure 2(a) gives the performance comparisons between different methods in terms of the CPU time over SNR. The proposed algorithm

[3] Code available in `http://ranger.uta.edu/~huang/R_CSMRI.htm`

is always the best, by achieving the highest SNR in less CPU time. The FCSA is always inferior to the proposed FCSA-MT, which shows the effectiveness of simultaneous reconstruction for multi-contrast MRI.

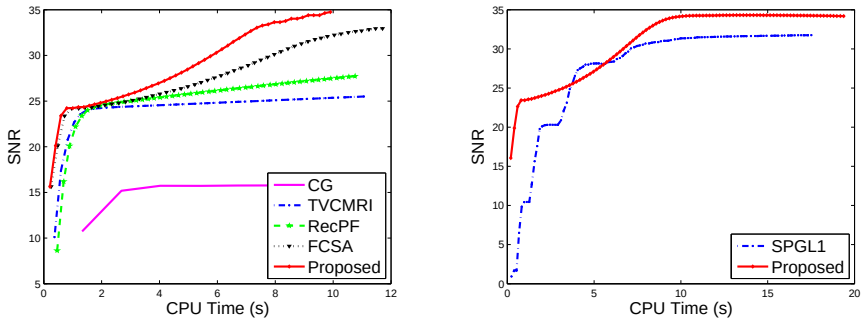

(a) (b)

Fig. 2: Performance comparisons (CPU-Time vs. SNR): a) Conventional CS-MRI, CG [2], TVCMRI [3],RecPF [4] and FCSA [5]; b) Multi-contrast CS-MRI:SPGL1 [8] vs. Proposed.

We then compared the proposed method with two multi-contrast reconstruction methods (SPGL1 [8] and Bayesian [9]) on all images. The sample ratio was set to be approximately 25%. To reduce the randomness, each experiment ran 100 times for each parameter setting of each method. Figure 2(b) gives the performance comparisons between the proposed method and SPGL1 [8] in terms of the CPU time vs. SNR. The proposed algorithm is always better, by achieving the higher SNR in less CPU time. As the Bayesian method is too slow, we resized the images to 128×128. Table 1 tabulates the comparison between the Bayesian method [9] and the proposed method on all images. Besides SNR, mean Structural Similarity (MSSIM) [14] is also considered for result evaluation. The proposed method is always best, in terms of both reconstruction accuracy and computational complexity. These results are reasonable, as we consider group sparsity on both wavelet domain and gradient domain while others only exploit one of them. This clearly demonstrates its effectiveness and efficiency for multi-contrast reconstruction.

5 Conclusion

We have proposed an efficient algorithm for multi-contrast CS-MRI. The contributions of our work are as follows. First, the proposed FCSA-MT achieves the best reconstruction performance over all previous methods. Second, the computational cost of the proposed method is only $\mathcal{O}(Tn\log(n))$ in each iteration. It can obtain an ϵ-optimal solution in $\mathcal{O}(1/\sqrt{\epsilon})$ iterations. These properties make

Table 1: Bayesian [9] vs. Proposed for Multi-contrast CS-MRI

	Bayesian [9]					Proposed				
Iterations	1000	1500	2000	2500	3000	10	15	20	25	30
Time (s)	144	305	516	829	1199	0.4	0.5	0.7	0.9	1.1
SNR (db)	24.9	25.2	27.9	28.3	29.1	25.4	29.7	30.9	31.1	31.2
MSSIM (%)	97.75	98.62	99.05	99.30	99.47	93.32	98.75	99.25	99.44	99.63

real-time multi-contrast CS-MRI much more feasible than before. Finally, numerous experiments were conducted to show that the proposed method outperforms all conventional CS-MRI methods and two recent multi-contrast CS-MRI methods in terms of accuracy and complexity.

References

1. Donoho, D.: Compressed sensing. IEEE Transactions on Information Theory **52**(4) (2006) 1289–1306
2. Lustig, M., Donoho, D., Pauly, J.: Sparse MRI: The application of compressed sensing for rapid mr imaging. Magnetic Resonance in Medicine **58** (2007) 1182–1195
3. Ma, S., Yin, W., Zhang, Y., Chakraborty, A.: An efficient algorithm for compressed MR imaging using total variation and wavelets. In: Proceedings of CVPR. (2008)
4. Yang, J., Zhang, Y., Yin, W.: A fast alternating direction method for TVL1-L2 signal reconstruction from partial fourier data. IEEE Journal of Selected Topics in Signal Processing, Special Issue on Compressive Sensing **4**(2) (2010)
5. Huang, J., Zhang, S., Metaxas, D.: Efficient MR image reconstruction for compressed MR imaging. In: Proceedings of MICCAI. (2010)
6. Huang, J., Zhang, S., Metaxas, D.: Efficient MR image reconstruction for compressed MR imaging. Medical Image Analysis **15** (2011) 670–679
7. Huang, J., Zhang, T.: The benefit of group sparsity. Annals of Statistics **38** (2010) 1978–2004
8. Majumdar, A., Ward, R.: Joint reconstruction of multiecho MR images using correlated sparsity. Magnetic Resonance Imaging **29** (2011) 899–906
9. Bilgic, B., Goyal, V., Adalsteinsson, E.: Multi-contrast reconstruction with bayesian compressed sensing. Magnetic Resonance Medicine **66** (2011) 1601–1615
10. Ji, S., Dunson, D., Carin, L.: Multitask compressive sensing. IEEE Transactions on Signal Processing **57** (2009) 92–106
11. Berg, E., Friedlander, M.: Probing the pareto frontier for basis pursuit solutions. SIAM Journal on Scientific Computing **31** (2008) 890–912
12. Beck, A., Teboulle, M.: Fast gradient-based algorithms for constrained total variation image denoising and deblurring problems. IEEE Transaction on Image Processing **18**(113) (2009) 2419–2434
13. Rohlfing, T., NM, N.Z., Sullivan, E., Pfefferbaum, A.: The sri24 multichannel atlas of normal adult human brain structure. Human Brain Mapping **31** (2010) 798–819
14. Wang, Z., Bovik, A.C., Sheikh, H.R., Simoncelli, E.P.: Image quality assessment: From error measurement to structural similarit. IEEE Transactions on Image Processing **13**(4) (2004) 600–612